J Shoulder Elbow Surg (2021) 30, 421–429

ELSEVIER

Journal of Shoulder and Elbow Surgery

www.elsevier.com/locate/ymse

In vivo reverse total shoulder arthroplasty contact mechanics

Madeleine L. Van de Kleut, BMSc[a,b,c,*], Chaithanya Nair[d], Jaques S. Milner, BESc[a], David W. Holdsworth, PhD[a,e], George S. Athwal, MD, FRCSC[c,f], Matthew G. Teeter, PhD[a,c,e,f]

[a]*Imaging Research Laboratories, Robarts Research Institute, London, ON, Canada*
[b]*School of Biomedical Engineering, Western University, London, ON, Canada*
[c]*Lawson Health Research Institute, London, ON, Canada*
[d]*Faculty of Science, Western University, London, ON, Canada*
[e]*Department of Medical Biophysics, Schulich School of Medicine and Dentistry, Western University, London, ON, Canada*
[f]*Roth|McFarlane Hand and Upper Limb Center, Department of Surgery, Schulich School of Medicine and Dentistry, Western University, London, ON, Canada*

Background: Several in vitro studies have investigated the biomechanics of reverse total shoulder arthroplasty (RTSA); however, few in vivo studies exist. The purpose of this study was to examine in vivo RTSA contact mechanics in clinically relevant arm positions. Our hypothesis was that contact would preferentially occur in the inferior region of the polyethylene liner.
Methods: Forty patients receiving a primary RTSA were recruited for a prospective cohort study. All patients received the same implant design with a nonretentive liner. Stereo radiographs were taken at maximal active range of motion. Model-based radiostereometric analysis was used to identify implant position. Contact area between the polyethylene and glenosphere was measured as the geometric intersection of the 2 components and compared with respect to polyethylene liner size, arm position, and relative position within the liner.
Results: There were no differences in the proportion of contact area in any arm position between polyethylene liner sizes, ranging from 30% ± 17% to 38% ± 23% for 36-mm liners and 32% ± 21% to 41% ± 25% for 42-mm liners. Contact was equally distributed between the superior and inferior halves of the liner at each arm position ($P = .06$-$.79$); however, greater contact area was observed in the outer radius of the liner when the arm was flexed ($P = .002$).
Conclusion: This study highlights that contact mechanics are similar between 36- and 42-mm liners. Contact area is generally equally distributed throughout the liner across the range of motion and not preferentially in the inferior region as hypothesized.
Level of evidence: Basic Science Study; Kinesiology

Keywords: Reverse total shoulder arthroplasty; contact mechanics; biomechanics; radiostereometric analysis; BIO-RSA; glenosphere lateralization

The unconventional design of reverse shoulder prostheses has prompted a number of biomechanical investigations to enhance the understanding of its mechanism of action. Finite element and cadaveric studies have assessed joint reaction forces generated during flexion and abduction

This study was approved by the Western University Health Sciences Research Ethics Board (project ID 105908).

*Reprint requests: Madeleine L. Van de Kleut, BMSc, Western University, 339 Windermere Road, London, ON, Canada N6A 5A5.
E-mail address: mvandekl@uwo.ca (M.L. Van de Kleut).

1058-2746/$ - see front matter Crown Copyright © 2020 All rights reserved.
https://doi.org/10.1016/j.jse.2020.05.036

while varying parameters such as glenosphere diameter, lateralization, screw number, and polyethylene cup depth in efforts to optimize function, minimize scapular notching, and maximize implant fixation.[8,15,16,21–23] Compared to native glenohumeral mechanics, these simulations suggest reduced compressive deltoid forces and increased shear forces during arm elevation, with joint loads that act on the lower half of the glenosphere.[1,16] The contact mechanics of various reverse total shoulder arthroplasty (RTSA) parameters were assessed in a finite element study using these results, where it was found that larger glenosphere diameters exhibited greater polyethylene contact area, and that focal stresses on the polyethylene were located in the inferior portion of the cup, indicating areas of possibly reduced mechanical integrity over time.[22] Larger glenosphere diameters have been proposed to increase range of motion,[10,24] though potentially at the cost of increased polyethylene wear[11,13] and without an observed reduction in maximum contact stress.[22]

Though simulation studies provide a fast and cost-effective evaluation of different implant designs, they are limited to controlled environments with predictable, repeatable conditions that may not be able to replicate what is observed in vivo.[7] For this reason, we sought to assess RTSA contact mechanics in vivo as a surrogate for joint forces, at clinically relevant arm positions. This method of in vivo assessment has frequently been used in total knee arthroplasty to evaluate the effect of different implant designs and surgical techniques on joint contact during activities of daily living,[6,12,26,29] where atypical contact patterns can be indicative of component migration and wear.[27,31] Our goal was to understand contact mechanics early after implantation, such that values would not be affected by polyethylene wear or damage. The purpose of this study was to answer 3 questions: (1) Is there a difference in contact area between 36- and 42-mm polyethylene liners; (2) does the magnitude of contact area change with different arm positions; and (3) does the location of the contact area change with these different arm positions? It was hypothesized that (1) 42-mm polyethylene liners would demonstrate greater contact area than 36-mm liners; (2) the normalized contact area would not change with different arm positions; and (3) that contact area would be eccentrically located within the liner during flexion and localized to the inferior portion of the liner for all arm positions.

Materials and methods

Patient recruitment

This is a prospective, cohort study, conducted as a secondary outcome measure to a randomized clinical trial investigating glenosphere migration between bony increased-offset reverse shoulder arthroplasty (BIO-RSA) and porous metal wedge augmented glenoid baseplates. Included with the informed consent of the primary randomized trial was consent to participate in this study investigating RTSA contact mechanics. All procedures were approved by the local institutional review board prior to patient enrollment.

Forty nonconsecutive participants were recruited, following power analysis for the randomized trial, and surgery was performed by a single fellowship-trained surgeon (G.S.A.) between July 2017 and June 2019. Inclusion criteria were patients able to provide written informed consent, willing to undergo primary RTSA with implantation with 16 tantalum beads, and to undergo routine follow-up radiostereometric radiographs. Potential participants were excluded if their indication for surgery was fracture, revision arthroplasty, post-traumatic arthritis, or avascular necrosis; if they presented with insufficient bone quality; had evidence of cognitive decline; were pregnant or planning to become pregnant; or were unable to read or write English.

All patients received the Aequalis Ascend Flex humeral stem with a 145° neck-shaft angle and a nonretentive polyethylene liner (Wright Medical-Tornier Group, Memphis, TN, USA); the distribution of liner sizes are reported in Table I. Nineteen patients received an Aequalis Reversed II glenoid (BIO-RSA) and 21 received an Aequalis PerFORM Reversed porous metal augmented wedge (Wright Medical-Tornier Group).

Clinical outcomes

Presurgery and 3 months postoperatively, patients completed the American Shoulder and Elbow Surgeons Standardized Shoulder Assessment Form; Simple Shoulder Test; Subjective Shoulder Value; Disabilities of the Arm, Shoulder, and Hand questionnaire; Constant Shoulder score; and ranked their pain from 0-10. Maximal active flexion in the sagittal plane, abduction in the coronal plane, and adducted external rotation were recorded using a manual long-arm goniometer (Prestige Medical, Northridge, CA, USA). Internal rotation was recorded as the highest point along the spine with the thumb pointing upward, with numeric values assigned to the thresholds of the Constant Shoulder score—lateral thigh (1), buttock (2), lumbosacral junction (3), waist (4), T12 (5), and interscapular (6).

Imaging

Three months postoperatively, patients were brought to a dedicated radiostereometric analysis suite for imaging. Patients were seated in front of a uniplanar calibration cage (Cage 43; RSA Biomedical, Umea, Sweden), with exposures taken with the arm at the side, and at the limits of their range of motion in flexion, abduction, adducted external rotation, and internal rotation, for a total of 5 sets of radiographs. Exposures were taken at 90 kVp, ranging from 8.0-16.0 mAs, for optimal contrast while maintaining the ‘‘as low as reasonably achievable’’ principle. All patients attended the 3-month imaging session and completed the questionnaires.

Contact assessment

Radiographs were assessed in commercial model-based radiostereometric analysis (MBRSA) software (RSACore, Leiden,

Table I Patient demographics

Age at surgery, yr, mean ± SD	73 ± 8
Sex, n	
Female	18
Male	22
Glenosphere/polyethylene liner size, n	
36 mm	16
39 mm	6
42 mm	18
BIO-RSA, n	19
Wedge augment lateralization, n	21

SD, standard deviation; *BIO-RSA*, bony increased-offset reverse shoulder arthroplasty.

Netherlands). The contours from the glenosphere, humeral stem, and metaphyseal tray components were identified in each radiograph for each arm position, and contour-matching was used to position and orient the implant components in a global coordinate frame (Fig. 1, *a*), which has been validated for these reverse shoulder components.[14] Following MBRSA, the global position and orientation of the glenosphere, stem, and tray were recorded. These transformations were applied to CAD (computer-aided design) models of the implant components in a separate commercial software (Geomagic Studio, 3D Systems Inc., Morrisville, NC, USA) (Fig. 1, *b*). Because the polyethylene liner is not visible in the radiographs, no transformation for the liner was obtained through MBRSA. However, knowing that the liner lies flush with the metaphyseal tray, it was assumed that the transformations recorded for the tray would also apply to the liner. In this way, the polyethylene was virtually inserted into the stem-tray-poly ensemble for each patient, and this composite model was then used for contact assessment (Fig. 1, *c*). This technique has previously been applied in the lower limb to overcome polyethylene radiolucency in 2- and 3-dimensional registration.[20,32]

For each of the 5 arm positions, the transformed stem-tray-poly and glenosphere CAD models were opened in an in-house program made specifically for analyzing the contact between them (Fig. 2, *a*).[26] The composite model and glenosphere model were then discretized into voxels with length 0.150 mm. Euclidean distance transforms were used to measure the smallest distance between model boundary surfaces, measured as a surface normal from each glenosphere voxel to the corresponding polyethylene surface voxel (Fig. 2, *b*). Distances from the glenosphere to the polyethylene liner were mapped onto the liner surface model from the glenosphere distance transform, and contact area was computed as the area inside an iso-contour on the polyethylene surface extracted at the contact threshold value (Fig. 2, *c*). A contact threshold of 0.3 mm was used to account for variations in sizing between the manufactured insert and glenosphere and their CAD models, respectively,[25] and the repeatability of the MBRSA imaging technique for reverse total shoulder arthroplasty implant components.[14]

Contact area was recorded for each arm position independently, and a total contact map was created by overlaying these independent areas. Overlapping areas from different arm positions were only counted once, so as to avoid overestimation. To spatially quantify contact area, the polyethylene liner was divided into superior and inferior halves (Fig. 3, *a*), and further, into its superior, inferior, anterior, and posterior quadrants, after accounting for whether it was implanted on the left or right side of the body (Fig. 3, *b*). The liner was also divided into concentric inner and outer areas of equal magnitude, with the intention of identifying any eccentric loading patterns (Fig. 3, *c*).

Statistical analysis

Prior to contact assessment, range of motion was compared between the randomized lateralization groups using a 2-tailed *t* test to determine potential confounding factors in the contact analysis. The D'Agostino and Pearson omnibus test was used to assess normality for each group of results.

The total contact area from each patient was recorded in terms of magnitude and normalized to the total area of the polyethylene liner, reported as a percentage of the area covered. A 2-tailed *t* test was used to determine any difference in contact area magnitude or as a percentage of coverage between the 36-mm (n = 16) and 42-mm (n = 18) liners for each arm position, including the total contact coverage. The 39-mm liners were not included in statistical comparison, as there were only 6 patients with this size. To consider the potential effect of range of motion on contact area, maximal flexion, having the greatest difference between patients (range 40°-165°), was linearly regressed with the respective normalized contact coverage for each patient in that position.

The Kruskal-Wallis test with the Dunn test for multiple comparisons was applied to determine whether there were any differences in the magnitude of contact area, normalized to total liner area, between the different arm positions.

A 2-tailed *t* test was applied to determine any difference in the percentage coverage of superior and inferior halves at each arm position. Similarly, the Kruskal-Wallis test with the Dunn test for multiple comparisons was applied to determine whether the contact area from each respective arm position was greater within a specific quadrant of the polyethylene.

A 2-tailed *t* test was used to determine if contact from any of the different arm positions was eccentric, as would be observed if the majority of the contact was located within the outer concentric area of the articular surface.

Results

Full patient demographics and functional outcomes are presented in Tables I and II, respectively. There were no differences between BIO-RSA and porous metal wedge lateralization groups in terms of flexion ($P = .26$), abduction ($P = .24$), external rotation ($P > .99$), or internal rotation ($P = .91$) at the time of imaging. For this reason, it was deemed acceptable to combine both lateralization groups into a single cohort for subsequent analysis.

There was no difference in contact coverage, as a percentage of the total polyethylene articular surface in contact with the glenosphere, between the 36- and 42-mm liners for any arm position, though differences in contact area magnitude were observed in internal rotation ($P = .048$) and for the combined contact map ($P = .001$), where 42-mm liners demonstrated greater contact area than 36-mm liners (Table III). There was no relationship

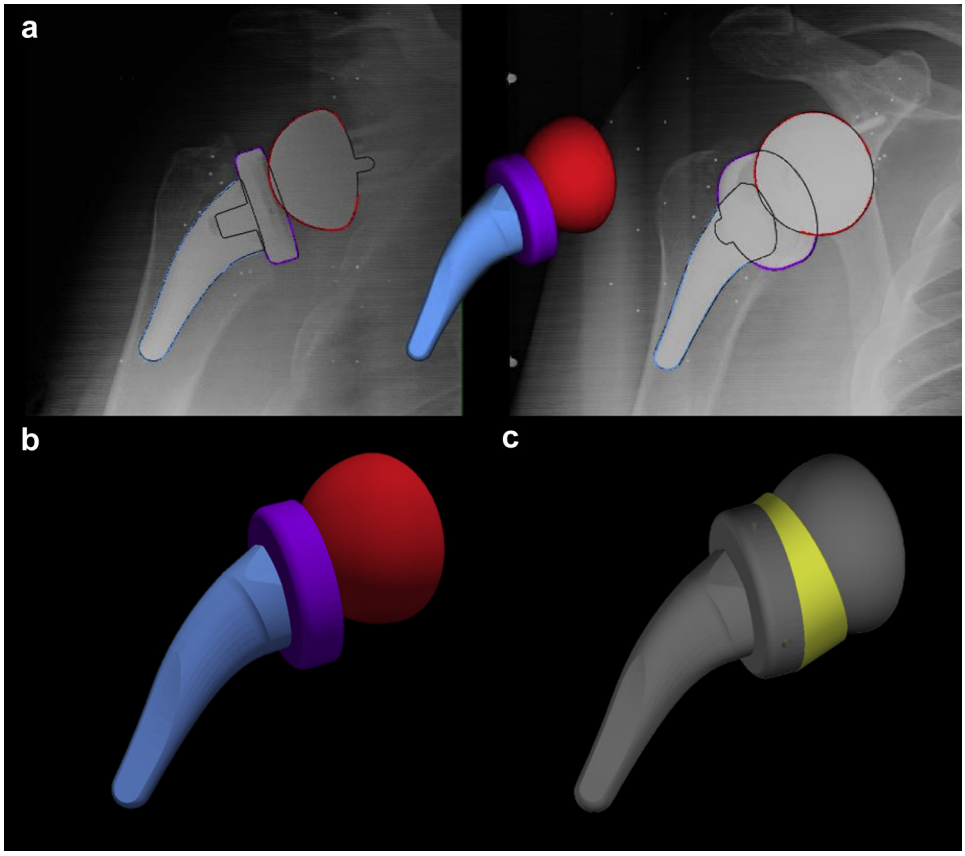

Figure 1 (**a**) Alignment of the stem (*blue*), tray (*purple*), and glenosphere (*red*) components in the model-based radiostereometric analysis software. The same transformations are applied to (**b**) the CAD models in Geomagic Studio, and (**c**) the polyethylene (*yellow*) virtually inserted in the tray.

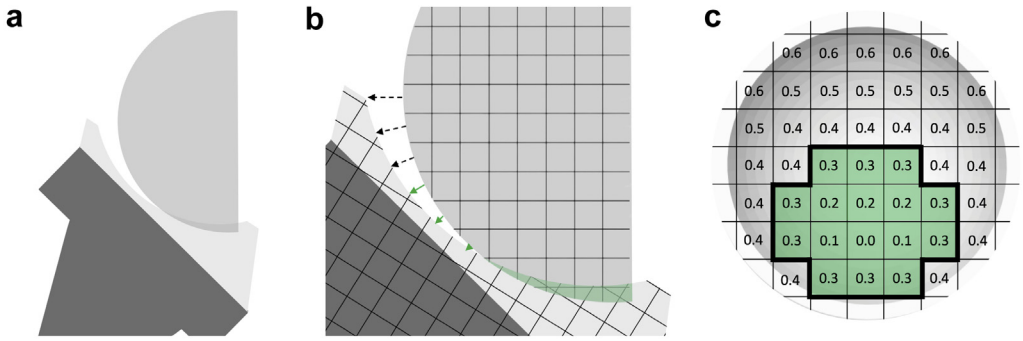

Figure 2 Contact area was measured by (**a**) importing the transformed composite and glenosphere models into an in-house software program, then (**b**) discretizing the models into voxels, whereby the distance between boundary surfaces was measured as the smallest distance from each glenosphere voxel to the polyethylene surface: distances greater than 0.3 mm (*dashed black arrows*) were excluded from the contact area measurement; distances less than or equal to 0.3 mm (*green arrows*), including intersection of the models (*green shaded area*), were included. (**c**) Distance from the glenosphere to the polyethylene surface was mapped to each polyethylene surface voxel, where voxels corresponding to distances less than or equal to the contact threshold were included in the area measurement.

between flexion and normalized contact coverage ($r^2 = 0.008$, $P = .61$).

As there were no observed statistical differences between the 2 liner sizes in terms of the normalized contact area, the 2 groups, with the addition of the 39-mm liner results, were combined into a single cohort to assess whether there were any differences in the normalized contact area between arm positions. All arm positions showed equal contact ($P = .99$) as a percentage of polyethylene area covered, with 33% ± 20% in the neutral and flexion positions, 34% ± 20% in abduction, 34% ± 24% in internal rotation, and 35% ± 20% in external rotation. The

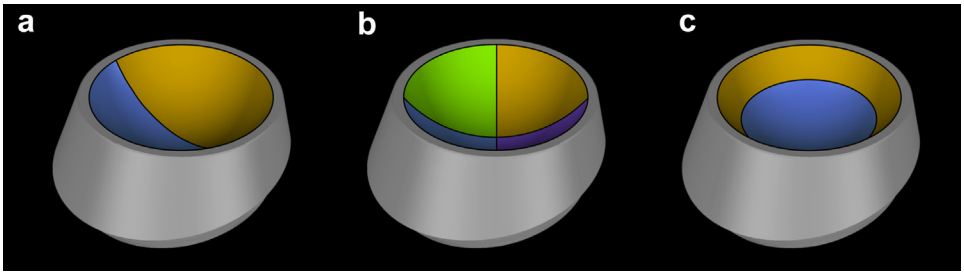

Figure 3 The polyethylene was divided into (**a**) superior (*orange*) and inferior (*blue*) halves, (**b**) quadrants of equal surface area, and (**c**) into inner (*blue*) and outer (*orange*) articular surfaces of equal surface area.

Table II Active range of motion and patient-reported outcome measures

	Preoperative* mean ± SD	3-mo postoperative* mean ± SD	*P* value
Flexion (°)	73 ± 28	96 ± 29	<.001
Abduction (°)	65 ± 24	86 ± 24	<.001
External rotation (°)	25 ± 21	26 ± 16	.73
Internal rotation†	3 ± 2	3 ± 2	.79
ASES (/100)	33.7 ± 16.3	62.0 ± 17.1	<.001
Pain (/10)	7.0 ± 2.3	2.9 ± 2.2	<.001
SSV (/100)	31± 21 (n = 22)	66 ± 21 (n = 36)	<.001
SST (/12)	2.4 ± 2.0	4.7 ± 3.0	<.001
DASH (/100)	54.1 ± 15.8	42.7 ± 18.8 (n = 39)	.004
Constant (/100)	26.6 ± 13.0	49.1 ± 15.5 (n = 39)	<.001

ASES, American Shoulder and Elbow Surgeons Standardized Shoulder Assessment Form; *SSV*, Subjective Shoulder Value; *SST*, Simple Shoulder Test; *DASH*, Disabilities of the Arm, Shoulder, and Hand questionnaire; *SD*, standard deviation.

* n = 40 unless otherwise indicated.

† Values assigned as lateral thigh = 1, buttock = 2, lumbosacral junction = 3, waist = 4, T12 = 5, and T7 = 6.

contact maps from each patient for each arm position, in addition to the combined contact map, were overlaid and normalized to polyethylene liner size to visualize contact within the liner (Fig. 4, *a-f*). Increased opacity represents increased overlap between patients.

There were no significant ($P > .06$) differences in how much contact was observed on either the superior or inferior half of the polyethylene at any arm position (Table IV).

Comparing the proportion of each quadrant in contact during different arm positions, the only significant difference was observed for internal rotation, where there was significantly greater contact in the inferior ($P = .015$) and posterior ($P = .026$) quadrants compared with the superior quadrant (Table V).

The contact area was also divided based on the proportion that was observed on the inner and outer concentric articular surface. Contact was equally distributed within the articular surface, except for when the arm was in the flexion position, where there was significantly greater contact located within the outer area of the liner (Table VI).

Discussion

The purpose of this study was to evaluate the contact mechanics of the reverse shoulder in vivo. Component contact has been investigated in total knee arthroplasty, where atypical contact patterns were associated with eccentric loading, the potential for premature wear, and continuous implant migration.[26–28] There is a paucity of literature related to reverse total shoulder arthroplasty contact mechanics, and to our knowledge this is one of the first vivo studies.

Our results highlight that over all ranges of shoulder motion, approximately 60% of the 36-mm liner and 70% of the 42-mm liner articular surface had contact. Although no significant differences were observed in the normalized contact area between liner sizes, the 42-mm liner demonstrated greater total contact area in terms of magnitude, partially supporting our first hypothesis. These trends are similar to what was predicted by Langohr et al,[22] where increasing glenosphere size increased contact area. In contrast to this simulation, however, it is interesting to note that contact was distributed between both superior and inferior halves of the polyethylene for each arm position, and at any one instance, approximately 30%-40% of the polyethylene was in contact with the glenosphere, supporting our second hypothesis but challenging the notion that contact is localized to the inferior portion of the liner. All patients in this study had some form of glenosphere lateralization, either through BIO-RSA or with porous metal wedge augmentation, with the premise of improving

Table III Contact coverage for 36- and 42-mm polyethylene liners

Arm position	% Poly contact 36 mm, mean ± SD	% Poly contact 42 mm, mean ± SD	*P* value	36-mm contact area, mm^2, mean ± SD	42-mm contact area, mm^2, mean ± SD	*P* value
Neutral	30 ± 17	32 ± 21	.93	346 ± 194	457 ± 303	.35
External rotation	38 ± 23	37 ± 16	.88	428 ± 259	525 ± 227	.26
Internal rotation	32 ± 23	41 ± 25	.28	360 ± 260	590 ± 365	**.048**
Flexion	32 ± 25	34 ± 16	.79	359 ± 287	483 ± 228	.20
Abduction	32 ± 19	37 ± 21	.43	360 ± 221	537 ± 305	.07
Combined	60 ± 21	69 ± 17	.19	687 ± 245	995 ± 250	**.001**

Poly, polyethylene liner; *SD*, standard deviation.

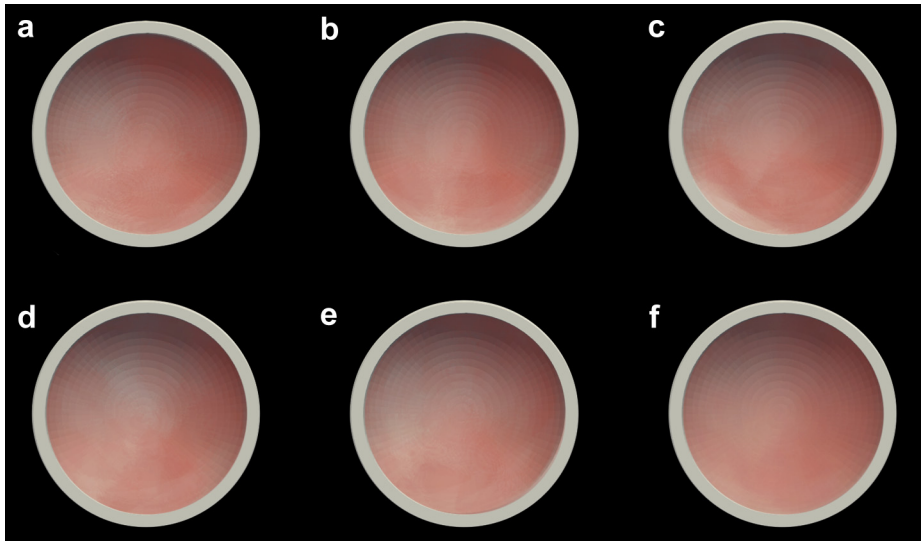

Figure 4 Contact area distribution (*red*) in the (**a**) neutral, (**b**) external rotation, (**c**) internal rotation, (**d**) flexion, and (**e**) abduction arm positions, and the (**f**) combined contact map. The anterior quadrant is represented on the left-hand side of the liner, the posterior quadrant on the right, and the superior quadrant is superior.

Table IV Proportion of superior and inferior halves in contact for different arm positions

Arm position	Superior, mean ± SD	Inferior, mean ± SD	*P* value
Neutral	31 ± 26	35 ± 23	.55
External rotation	33 ± 24	38 ± 23	.36
Internal rotation	28 ± 28	40 ± 25	.06
Flexion	28 ± 24	37 ± 26	.15
Abduction	32 ± 27	36 ± 25	.40
Combined	63 ± 28	68 ± 20	.79

SD, standard deviation.

impingement-free range of motion.[4,5,9] This lateralization, in addition to the 145° neck-shaft angle, may have resulted in more centrally located contact patches, as there was a frequent occurrence of polyethylene "underhang" in the neutral and externally rotated arm positions, as observed in Fig. 5.

Separating the contact into quadrants, the only instance of unequal contact was during internal rotation, where contact was significantly greater in the inferior and posterior quadrants. This particular instance of localized contact may contribute to polyethylene wear and merits further investigation.

When separating contact into contributions from the inner and outer aspects of the articular surface, there was a trend toward increased contact within the outer aspect of the liner, though the only significant difference was during flexion, where approximately 63% of the contact area in this position was within the outer area, partially supporting our third hypothesis. These results reflect the modeling study conducted by Kontaxis et al,[15] where they found that contact forces during activities of daily living were constrained within the stability of the rim, as well as the

Table V Proportion of each quadrant area in contact for different arm positions

Arm position	Superior, mean ± SD	Inferior, mean ± SD	Anterior, mean ± SD	Posterior, mean ± SD	*P* value
Neutral	30 ± 30	35 ± 27	26 ± 32	42 ± 31	.08
External rotation	30 ± 27	36 ± 28	34 ± 35	38 ± 34	.69
Internal rotation	23 ± 30	41 ± 29	28 ± 27	43 ± 36	**.004**
Flexion	24 ± 29	38 ± 32	29 ± 34	41 ± 34	.14
Abduction	30 ± 32	38 ± 30	30 ± 32	38 ± 34	.44
Combined	61 ± 32	68 ± 23	63 ± 32	69 ± 30	.38

SD, standard deviation.

Table VI Proportion of contact within the inner and outer articular surface for different arm positions

Arm position	% Inner contact, mean ± SD	% Outer contact, mean ± SD	*P* value
Neutral	44 ± 19	56 ± 19	.08
External rotation	43 ± 21	57 ± 21	.38
Internal rotation	47 ± 19	53 ± 19	.83
Flexion	37 ± 22	63 ± 22	**.002**
Abduction	43 ± 19	57 ± 19	.18
Combined	48 ± 7	52 ± 7	.25

SD, standard deviation.

cadaveric study by Ackland et al,[1] where they observed greater shear forces in flexion.

There are a number of factors contributing to the comparatively large standard deviations observed in this study. Most obviously, there were large differences in active range of motion between patients. This is likely because values for range of motion were taken at 3 months postoperatively, when patients are still improving. Our reasoning for acquiring measurements early was to determine the contact mechanics before any polyethylene wear or damage had occurred. Differences in muscle activation and resulting joint compression may also contribute to the variable contact patterns. It is interesting to note that between patients, the entire liner interacts with the glenosphere, and not only its inferior area, as previously hypothesized.[22]

Though measuring contact at the extents of patients' range of motion provides valuable information regarding the static location and magnitude of contact, dynamic fluoroscopic imaging for a variety of motion patterns related to activities of daily living could enhance our understanding of polyethylene-glenosphere sliding patterns and identify areas on the liner with the potential for excess wear. It should also be noted that contact area is separate from contact stress, where contact stress is a measure of force per unit area. A limitation of this study is that contact stress was not recorded, as measuring joint loads in vivo requires instrumented implants. It is also possible that patients with similar contact patterns experienced different contact stresses as a result of the use of a contact threshold—one would theorize that a patient with a smaller distance between the glenosphere and polyethylene liner would experience higher contact stresses than a patient with the same contact area but a larger distance between the glenosphere and liner. We therefore were unable to conclude whether participants with less contact area experienced higher contact stresses. It is interesting to note, however, that a finite element study conducted by Langohr et al[22] found that increasing glenosphere diameter increased joint loads during active abduction, and no appreciable reduction in contact stress was observed despite increases in contact area. This is important for simulation studies investigating the effects of different implant designs on wear, which has been shown to be non-negligible in the reverse shoulder.[13] Future studies could apply the relative positions of implants measured using model-based radiostereometric analysis within finite element analysis to observe the pattern and magnitude of contact stresses in the in vivo environment.

Further limitations to this study include the use of a single reverse shoulder arthroplasty model, including neck-shaft angle, and for this reason the results may not be directly applicable to all reverse total shoulder arthroplasty designs. Images were taken 3 months postoperatively, and as a result there was great diversity in the range of arm motions achieved by each patient. This variation, however, highlights the fact that contact may not be predictable even within a single reverse shoulder design. Future studies

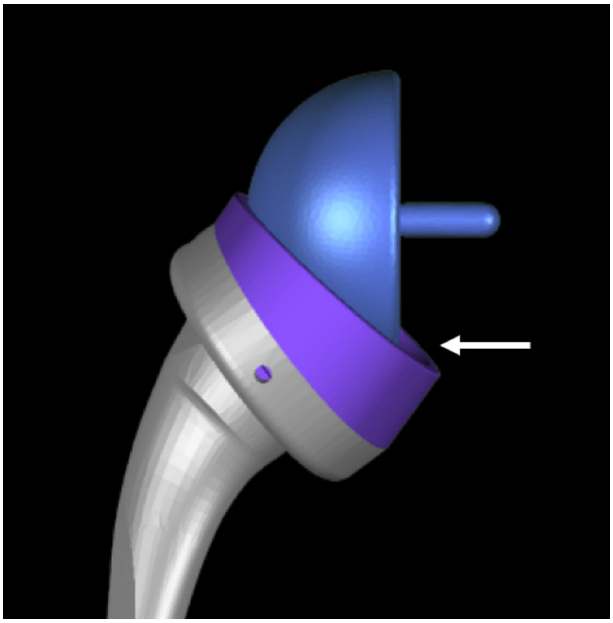

Figure 5 Example of polyethylene (*purple*) underhang relative to the glenosphere (*blue*) in the externally rotated arm position, indicated by the *white arrow*.

could enforce a standardized set of motions between patients, such as abduction at 90° rather than maximal abduction, to reduce interpatient variability when analyzing results.

The concept of using surface separation distance for measuring joint contact was initially introduced for the lower limb, but has more recently been applied in the biomechanical assessment of both the native joint and joint replacement in the upper limb with excellent validity.[2,3,17–19] The contact threshold of 0.3 mm was chosen to account for the variations in surface deviations observed between polyethylene liners and the repeatability of the model-based radiostereometric analysis technique[14,25]; however, changing this threshold would provide different results. Increasing the contact threshold would result in a greater perceived contact area, whereas decreasing the contact threshold has the potential to underestimate the contact. Future studies may consider the effect of contact threshold by performing a sensitivity analysis, validated using in vitro techniques such as pressure-sensitive film for a measure of true contact area.[2,30]

As previous studies of the lower limb have shown that atypical contact mechanics can lead to continuous implant migration and polyethylene wear,[26–28] there is the potential for other joint replacements to exhibit similar long-term behavior. It is therefore important to determine the range of normal contact patterns specific to different joint replacements. Patients who demonstrate atypical contact patterns and subsequently atypical joint loading may be at risk for future joint failure.[31] Future studies should investigate the long-term impact of contact mechanics on implant migration and polyethylene wear in order to classify contact patterns into those that are normal and those that may negatively influence long-term implant performance, potentially influencing future implant design.

Conclusion

The purpose of this study was to assess the in vivo contact mechanics of RTSA. The results highlight that contact mechanics are similar between 36- and 42-mm liners. Additionally, contact area is generally equally distributed throughout the polyethylene liner during early active range of motion and not preferentially in the inferior region as previously hypothesized.

Disclaimer

This study was funded by a grant from the Canadian Institutes of Health Research (FDN-14874), and the Ontario Research Fund—Research Excellence.

George S. Athwal has received research support funding, intellectual property royalties, and stock or stock options from Wright Medical Group Inc. No company had any input into the study design, protocol, testing, data analysis, or manuscript preparation. All the other authors, their immediate families, and any research foundations with which they are affiliated have not received any financial payments or other benefits from any commercial entity related to the subject of this article.

Acknowledgments

The authors thank Rudy Baronette for his assistance as x-ray technician for this study.

References

1. Ackland DC, Roshan-Zamir S, Richardson M, Pandy MG. Muscle and joint-contact loading at the glenohumeral joint after reverse total shoulder arthroplasty. J Orthop Res 2011;29:1850-8. https://doi.org/10.1002/jor.21437
2. Ateshian GA, Kwak SD, Soslowsky LJ, Mow VC. A stereophotogrammetric method for determining in situ contact areas in diarthrodial joints, and a comparison with other methods. J Biomech 1994;27:111-24.
3. Ateshian GA, Soslowsky LJ, Mow VC. Quantitation of articular surface topography and cartilage thickness in knee joints using stereophotogrammetry. J Biomech 1991;24:761-76.
4. Athwal GS, MacDermid JC, Reddy KM, Marsh JP, Faber KJ, Drosdowech D. Does bony increased-offset reverse shoulder arthroplasty decrease scapular notching? J Shoulder Elbow Surg 2015;24:468-73. https://doi.org/10.1016/j.jse.2014.08.015

5. Boileau P, Morin-Salvo N, Gauci MO, Seeto BL, Chalmers PN, Holzer N, et al. Angled BIO-RSA (bony-increased offset-reverse shoulder arthroplasty): A solution for the management glenoid bone loss and erosion. J Shoulder Elbow Surg 2017;26:2133-42. https://doi.org/10.1016/j.jse.2017.05.024
6. Broberg JS, Ndoja S, MacDonald SJ, Lanting BA, Teeter MG. Comparison of contact kinematics in posterior-stabilized and cruciate-retaining total knee arthroplasty at long-term follow-up. J Arthroplasty 2019;74:1-12. https://doi.org/10.1016/j.arth.2019.07.046
7. Cooper RJ, Wilcox RK, Jones AC. Finite element models of the tibiofemoral joint: a review of validation approaches and modelling challenges. Med Eng Phys 2019;74:1-12. https://doi.org/10.1016/j.medengphy.2019.08.002
8. Elwell J, Choi J, Willing R. Quantifying the competing relationship between adduction range of motion and baseplate micromotion with lateralization of reverse total shoulder arthroplasty. J Biomech 2017;52:24-30. https://doi.org/10.1016/j.jbiomech.2016.11.053
9. Gutiérrez S, Comiskey CAIV, Luo ZP, Pupello DR, Frankle MA. Range of impingement-free abduction and adduction deficit after reverse shoulder arthroplasty: hierarchy of surgical and implant-design-related factors. J Bone Joint Surg Am 2008;90:2606-15. https://doi.org/10.2106/JBJS.H.00012
10. Gutiérrez S, Levy JC, Frankle MA, Cuff D, Keller TS, Pupello DR, et al. Evaluation of abduction range of motion and avoidance of inferior scapular impingement in a reverse shoulder model. J Shoulder Elbow Surg 2008;17:608-15. https://doi.org/10.1016/j.jse.2007.11.010
11. Haggart J, Newton MD, Hartner S, Ho A, Baker KC, Kurdziel MD, et al. Neer Award 2017: Wear rates of 32-mm and 40-mm glenospheres in a reverse total shoulder arthroplasty wear simulation model. J Shoulder Elbow Surg 2017;26:2029-37. https://doi.org/10.1016/j.jse.2017.06.036
12. Horsager K, Kaptein BL, Jørgensen PB, Jepsen CF, Stilling M. Oxford medial unicompartmental knees display contact-loss during step-cycle motion and bicycle motion: a dynamic radiostereometric study. J Orthop Res 2018;36:357-64. https://doi.org/10.1002/jor.23625
13. Van de Kleut ML, Athwal GS, Faber KJ, Teeter MG. In vivo volumetric and linear wear measurement of reverse shoulder arthroplasty at minimum 5-year follow-up. J Shoulder Elbow Surg 2020;29:1695-702. https://doi.org/10.1016/j.jse.2019.11.031
14. Van de Kleut ML, Yuan X, Athwal GS, Teeter MG. Validation of radiostereometric analysis in six degrees of freedom for use with reverse total shoulder arthroplasty. J Biomech 2018;68:126-31. https://doi.org/10.1016/j.jbiomech.2017.12.027
15. Kontaxis A, Johnson GR. The biomechanics of reverse anatomy shoulder replacement—a modelling study. Clin Biomech 2009;24:254-60. https://doi.org/10.1016/j.clinbiomech.2008.12.004
16. Kwon YW, Forman RE, Walker PS, Zuckerman JD. Analysis of reverse total shoulder joint forces and glenoid fixation. Bull NYU Hosp Jt Dis 2010;68:273-80.
17. Lalone EA, Grewal R, MacDermid JC. Impact of radius malunion on wrist contact mechanics. J Orthop Sports Phys Ther 2016;46:399. https://doi.org/10.2519/jospt.2016.0406
18. Lalone EA, McDonald CP, Ferreira LM, Peters TM, King GW, Johnson JA. Development of an image-based technique to examine joint congruency at the elbow. Comput Methods Biomech Biomed Engin 2013;16:280-90. https://doi.org/10.1080/10255842.2011.617006
19. Lalone EA, Shannon HL, Deluce SR, Giles JW, King GJW, Johnson JA. Effect of radial head implant shape on radiocapitellar joint congruency. J Hand Surg Am 2017;42:476.e1-e11. https://doi.org/10.1016/j.jhsa.2017.03.009
20. Lam-Tin-Cheung K, Yuan X, Nikolov HN, Lanting BA, Naudie DD, Teeter MG. Marker-based technique for visualizing radiolucent implant components in radiographic imaging. J Orthop Res 2017;35:2017-22. https://doi.org/10.1002/jor.23475
21. Langohr GDG, Giles JW, Athwal GS, Johnson JA. The effect of glenosphere diameter in reverse shoulder arthroplasty on muscle force, joint load, and range of motion. J Shoulder Elbow Surg 2015;24:972-9. https://doi.org/10.1016/j.jse.2014.10.018
22. Langohr GDG, Willing R, Medley JB, Athwal GS, Johnson JA. Contact mechanics of reverse total shoulder arthroplasty during abduction: the effect of neck-shaft angle, humeral cup depth, and glenosphere diameter. J Shoulder Elbow Surg 2016;25:589-97. https://doi.org/10.1016/j.jse.2015.09.024
23. Liou W, Yang Y, Petersen-Fitts GR, Lombardo DJ, Stine S, Sabesan VJ. Effect of lateralized design on muscle and joint reaction forces for reverse shoulder arthroplasty. J Shoulder Elbow Surg 2017;26:564-72. https://doi.org/10.1016/j.jse.2016.09.045
24. Müller AM, Born M, Jung C, Flury M, Kolling C, Schwyzer HK, et al. Glenosphere size in reverse shoulder arthroplasty: is larger better for external rotation and abduction strength? J Shoulder Elbow Surg 2018;27:44-52. https://doi.org/10.1016/j.jse.2017.06.002
25. Teeter MG, Dawson MT, Athwal GS. Inter and intra-system size variability of reverse shoulder arthroplasty polyethylene inserts. Int J Shoulder Surg 2016;10:10-4. https://doi.org/10.4103/0973-6042.174512
26. Teeter MG, Perry KI, Yuan X, Howard JL, Lanting BA. Contact kinematic differences between gap balanced vs measured resection techniques for single radius posterior-stabilized total knee arthroplasty. J Arthroplasty 2017;32:1834-8. https://doi.org/10.1016/j.arth.2016.12.054
27. Teeter MG, Perry KI, Yuan X, Howard JL, Lanting BA. Contact kinematics correlates to tibial component migration following single radius posterior stabilized knee replacement. J Arthroplasty 2018;33:740-5. https://doi.org/10.1016/j.arth.2017.09.064
28. Vandekerckhove PJTK, Teeter MG, Naudie DDR, Howard JL, MacDonald SJ, Lanting BA. The impact of wear and lift-off on coronal plane alignment in TKA and implications to future constrained revision: a retrieval study. J Arthroplasty 2015;30:2017-20. https://doi.org/10.1016/j.arth.2015.05.048
29. Varadarajan KM, Moynihan AL, D'Lima D, Colwell CW, Li G. In vivo contact kinematics and contact forces of the knee after total knee arthroplasty during dynamic weight-bearing activities. J Biomech 2008;41:2159-68. https://doi.org/10.1016/j.jbiomech.2008.04.021
30. Villa T, Migliavacca F, Gastaldi D, Colombo M, Pietrabissa R. Contact stresses and fatigue life in a knee prosthesis: comparison between in vitro measurements and computational simulations. J Biomech 2004;37:45-53. https://doi.org/10.1016/S0021-9290(03)00255-0
31. Williams JL, Knox DA, Teeter MG, Holdsworth DW, Mihalko WM. Evidence that in vivo wear damage alters kinematics and contact stresses in a total knee replacement. J Long Term Eff Med Implants 2010;20:43-8. https://doi.org/10.1615/jlongtermeffmedimplants.v20.i1.60
32. Yamazaki T, Watanabe T, Nakajima Y, Sugamoto K, Tomita T, Maeda D, et al. Visualization of femorotibial contact in total knee arthroplasty using X-ray fluoroscopy. Eur J Radiol 2005;53:84-9. https://doi.org/10.1016/j.ejrad.2003.09.018